Physics Letters B 819 (2021) 136445

Contents lists available at ScienceDirect

Physics Letters B

www.elsevier.com/locate/physletb

Proton entropy excess and possible signature of pairing reentrance in hot nuclei

Balaram Dey [a], Srijit Bhattacharya [b], Deepak Pandit [c,d], N. Dinh Dang [e], N. Ngoc Anh [f], L. Tan Phuc [g,h], N. Quang Hung [g,h,*]

[a] Department of Physics, Bankura University, Bankura, West Bengal-722155, India
[b] Department of Physics, Barasat Govt. College, Barasat, N 24 Pgs, Kolkata-700124, India
[c] Variable Energy Cyclotron Centre, 1/AF-Bidhannagar, Kolkata-700064, India
[d] Homi Bhabha National Institute, Training School Complex, Anushaktinagar, Mumbai 400094, India
[e] Quantum Hadron Physics Laboratory, RIKEN Nishina Center for Accelerator-Based Science, 2-1 Hirosawa, Wako City, 351-0198 Saitama, Japan
[f] Dalat Nuclear Research Institute, Vietnam Atomic Energy Institute, 01 Nguyen Tu Luc, Dalat City 670000, Viet Nam
[g] Institute of Fundamental and Applied Sciences, Duy Tan University, Ho Chi Minh City 700000, Viet Nam
[h] Faculty of Natural Sciences, Duy Tan University, Da Nang City 550000, Viet Nam

ARTICLE INFO

Article history:
Received 28 April 2021
Received in revised form 1 June 2021
Accepted 8 June 2021
Available online 9 June 2021
Editor: Editor: W. Haxton

Keywords:
Nuclear level density
Proton entropy excess
Exact thermal pairing
Pairing reentrance

ABSTRACT

The entropy excess caused by one proton (proton entropy excess) has been extracted for several pairs of medium and heavy mass nuclei such as (^{237}U and ^{238}Np), (^{231}Th and ^{232}Pa), (^{211}Po and ^{212}At), (^{196}Pt and ^{197}Au), and (^{90}Y and ^{91}Zr) using the available nuclear level density data. The nature of entropy excess as a function of excitation energy E^* is found in a reasonable agreement with the microscopic calculations based on the exact pairing plus independent-particle model at finite temperature (EP+IPM). It is observed that the proton entropy excess is $\sim 0.1-0.5\ k_B$ for the spherical systems and $\sim 1.0-1.2\ k_B$ for the deformed ones, which is notably smaller than that of neutron entropy excess ($\sim 1.3-2.0\ k_B$). This is due to the effect of Coulomb interaction as well as the single-particle level density of protons, which is less than that of neutrons. Moreover, a peak-like structure in the entropy excess observed at low $E^* < 1$ MeV is possibly associated with the pairing reentrance phenomenon caused by the weakening of blocking effect in odd nuclei at low temperature within the EP+IPM. However, this peak-like structure, which is more pronounced in the spherical nuclei than in the deformed isotopes, is not well supported by experimental observation due to strong fluctuations of the measured data. Hence, further experimental and theoretical studies are called in order to understand this effect.

The atomic nucleus is only about 10^{-5} times the size of an atom. However, the study of thermodynamics of this minuscule fundamental piece of matter can provide us the much-needed clue to understand the evolution of gigantic universe as well as the thermal properties of small systems. The nuclear thermodynamics also play a leading role in the study of the nuclear equation of state (EOS). The low-temperature EOS enlightens us about cold neutron stars and nuclear superfluidity. On the contrary, the high-temperature EOS informs us the neutron star cooling, big bang nucleosynthesis (BBN), etc. [1,2]. The information on the entropy of nuclear matter and the contribution of each nucleon have immense potential in building up the model of BBN. The ratio of the number of photons in the universe to the number of baryons is proportional to the average thermal entropy. This ratio, which is about 10^9, provides an insight into the matter-antimatter asymmetry in the present universe [3,4]. Hence, the study of nuclear thermodynamics and entropy excess caused by a single nucleon in the nucleus is always one of the topics of much interest in nuclear physics and astrophysics.

Meanwhile, the heat capacity and entropy can be directly extracted from the nuclear level density (NLD), a quantity which can be experimentally measured. Based on the heat capacity and entropy, one can investigate some spectacular characteristics of small systems such as the pairing symmetry breaking as well as the associated pairing phase transition. For instance, the signature of discontinuity in the heat capacity curve, which is smoothed out by the statistical fluctuations inside the small system, or in other

* Corresponding author at: Institute of Fundamental and Applied Sciences, Duy Tan University, Ho Chi Minh City 700000, Viet Nam.
E-mail addresses: dey.balaram@gmail.com (B. Dey), srijit.bha@gmail.com (S. Bhattacharya), deepak.pandit@vecc.gov.in (D. Pandit), dang@riken.jp (N. Dinh Dang), ngocanh8999@gmail.com (N. Ngoc Anh), letanphuc2@dtu.edu.vn (L. Tan Phuc), nguyenquanghung5@duytan.edu.vn (N. Quang Hung).

https://doi.org/10.1016/j.physletb.2021.136445

words, the *S*-shaped heat capacity, can expose the pairing phase transition in the system, especially at low excitation energy E^* [5–11]. Furthermore, based on the heat capacity and entropy, one can also investigate the possible signature of the pairing reentrance phenomenon, which has been predicted in both hot [12–14] and hot rotating nuclei [15–21]. In hot rotating nuclei, this phenomenon occurs in such a way that, when the nucleus carries an angular momentum J slightly higher than a critical value J_c, its pairing correlation vanishes at low temperature $T \leq T_1$, increases at a certain $T > T_1$ to reach a maximum, and decreases to vanish again at $T \geq T_2$ [22–24]. When thermal fluctuations are taken into account in finite nuclei, the pairing reentrance phenomenon occurs in a slightly different way, namely the pairing gap reappears at a given T and remains finite at higher T due to the strong fluctuations of the order parameters [16–20]. In addition, the pairing reentrance can also be seen in hot even-even nuclei (without rotation), which are close to or beyond the drip line such as ^{48}Ni, ^{176}Sn, and ^{180}Sn [12,14]. This phenomenon has been explained by the fact that, in near or beyond the drip-line nuclei, the resonance states are often located at a relatively high energy at $T = 0$, preventing them to participate in pairing. These states, however, are close enough to the last occupied state, which could be reached at finite temperature and make pairing available [14]. In particular, pairing reentrance has been predicted to exist also in hot odd nuclei, but its behavior and nature are different from those in even systems, namely the pairing gap of odd nuclei, which is finite at $T = 0$, slightly increases at low $T \neq 0$, and decreases as T goes further. This occurs because of the weakening of the blocking effect caused by the odd nucleon in odd nuclei as explained in detail in Ref. [13].

Indeed, the heat capacity and entropy of nuclear many-body system have been calculated by using different models like the finite-temperature Hartree Fock (FTHF) [25], finite-temperature BCS (FTBCS) [23,24], relativistic mean field (RMF) [26,27], finite-temperature Hartree Fock Bogoliubov (FTHFB) [28,29], shell model Monte Carlo at finite temperature (SMMC) [30,31], exact pairing plus independent-particle model (EP+IPM) [32,33], etc. The information on the nuclear entropy, which can be calculated from the NLD by using the microcanonical ensemble [34,35], and the contribution of each nucleon have an immense potential in understanding different interesting phenomena associated with nuclear thermodynamics. Moreover, since the NLD is the product of all possible combinations of nucleons, the entropy contribution of a single nucleon can be studied by taking the entropy difference between two consecutive nuclei differing only by one nucleon. Thus, disentangling the role of a single nucleon in the entropy may provide the experimental signature of pairing phase transition and/or pairing reentrance in hot nuclei.

The microcanonical entropy had been previously estimated for $^{237-239}$U, $^{231-233}$Th [35], $^{195-196}$Pt, $^{197-198}$Au [36], $^{161-162}$Dy, $^{171-172}$Yb [37], $^{116-117}$Sn [38], and $^{56-57}$Fe [39] nuclei based on their experimental NLD data measured by using the Oslo technique [40]. It was found in these estimations that the entropy excess due to a single neutron ΔS_n stabilizes around $\Delta S_n \sim 1.3 - 2.0\ k_B$ at $E^* > 1 - 3$ MeV [35]. However, in the low-energy region $E^* \sim 0.7 - 1$ MeV, which is well below the energy needed to break the first neutron pair (about twice the neutron pairing gap), there appears a sharp peak in the distribution of ΔS_n (see e.g., Ref. [37]). This peak has not been discussed and/or explained by any theoretical model so far. Moreover, the entropy excess caused by a single proton (called as proton entropy excess hereafter) ΔS_p has not also been studied yet. Therefore, a systematic and elaborate investigation bearing nuclei of different properties is required to understand this topic.

In this Letter, a systematic study has been carried out to understand the proton entropy excess obtained for different pairs of odd-even and odd-odd nuclei ranging from A = 90 to 238 (^{90}Y and ^{91}Zr, ^{196}Pt and ^{197}Au, ^{211}Po and ^{212}At, ^{231}Th and ^{232}Pa, ^{237}U and ^{238}Np). The proton entropy excess determined from the existing experimental NLD data has been compared with the microscopic calculation within the EP+IPM. The latter has predicted an enhanced peak of ΔS_p at $E^* \sim 1$ MeV in near spherical nuclei (^{90}Y and ^{91}Zr, ^{211}Po and ^{212}At), indicating a possible signature of pairing reentrance in hot nuclei.

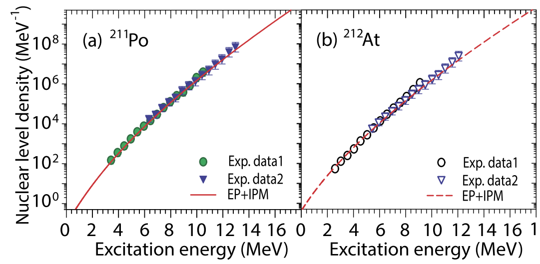

Fig. 1. Angular-momentum ($J \sim 12\hbar$) gated NLDs as functions of excitation energy E^* along with the EP+IPM NLDs for ^{211}Po (a) and ^{212}At (b) nuclei. The circles (Exp. data1) are taken from the our previous study [10], whereas the triangles (Exp. data2) represent the present NLDs extracted from the existing neutron energy spectra [41]. The EP+IPM NLDs are similar to those in [10] but with a slightly difference in their slope.

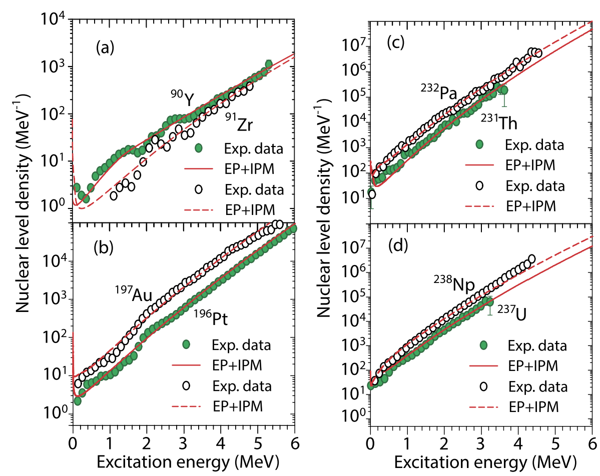

Fig. 2. NLDs as functions of excitation energy E^* along with the results of EP+IPM calculations for different nuclei. Experimental data are taken from Refs. [42] for ^{90}Y, [43] for ^{91}Zr, [36] for ^{196}Pt and ^{197}Au, [35] for ^{231}Th and ^{237}U, [44] for ^{232}Pa, and [45] for ^{238}Np.

Figs. 1 and 2 show the NLDs of all nuclei considered in the present Letter. In Figs. 1[(a) and (b)], the filled and opened circles denote, respectively, the NLDs of ^{211}Po and ^{212}At in the intermediate-energy region $E^* \sim 3 - 10$ MeV and at the total angular momentum $J \sim 12\ \hbar$ taken from our previous study [10], whereas the filled and opened triangles stand for the same NLDs but in a higher energy region ($E^* \sim 6 - 14$ MeV) extracted in the present work by using the neutron evaporation spectra. The latter are taken from Ref. [41] by employing the same procedure as discussed in our previous works [9,10]. In Fig. 2, the total NLDs of other mass regions are taken from the measurements by using the particle-γ coincidence measurements, e.g., ^{90}Y [42], ^{91}Zr [43], ^{196}Pt, ^{197}Au [36], ^{231}Th [35], ^{232}Pa [44], ^{237}U [35], and ^{238}Np [45]. To study the proton entropy excess, the nuclei are selected in such a way that two consecutive nuclei differ only by one proton. The experimental total and angular-momentum dependent NLDs are compared with those obtained by using the EP+IPM calculations. The formalism of the EP+IPM was described in detail in Refs. [9,10,32], so we do not repeat it here. The EP+IPM calculations are carried out based on the single-particle spectra taken

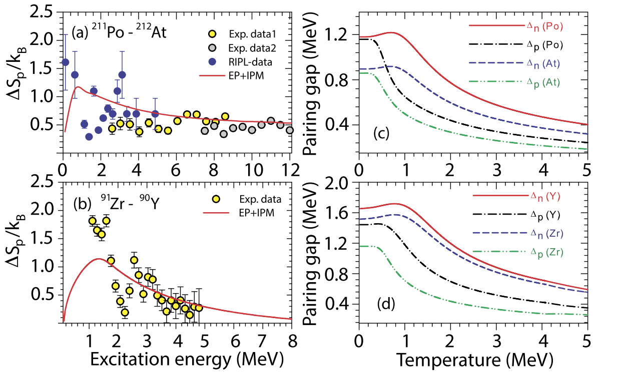

Fig. 3. [(a) and (b)] Proton entropy excesses ΔS_p as functions of excitation energy E^* along with the results of EP+IPM calculations for ^{211}Po–^{212}At and ^{90}Y–^{91}Zr. [(c) and (d)] Proton Δ_p and neutron Δ_n pairing gaps as functions of temperature T for different nuclei. Exp. data1 and Exp. data2 in (a) are obtained by using the associated NLD data (circles and triangles) in Fig. 1, respectively, whereas RIPL-data are calculated by using the low-energy data taken from RIPL-3 averaged over the angular-momentum distribution as in Ref. [10]. Exp. data in (b) are obtained by using the NLD data in Fig. 2(a).

from an axially deformed Woods-Saxon potential [46]. The values of the quadrupole deformation parameter β_2 for ^{196}Pt, ^{197}Au, ^{231}Th, ^{232}Pa, ^{237}U, and ^{238}Np are 0.130, -0.125, 0.195, 0.206, 0.226, and 0.226, respectively, whereas the β_2 values for ^{90}Y, ^{91}Zr, ^{211}Po, and ^{212}At are almost zero as they are spherical nuclei [47].

It is observed that the EP+IPM calculations very nicely reproduce the J-dependent NLD data (Figs. 1[(a) and (b)]) as well as the total NLDs (Fig. 2), confirming again the microscopic nature of the EP+IPM, as has been widely discussed in Refs. [9,10,32,48,49]. Knowing the NLD, one can easily calculate the entropy based on its definition in the microcanonical ensemble (MCE). The latter has been used in the present Letter because hot nuclei can be better described statistically through such an ensemble. Within this framework, the nucleus can be considered as an isolated system with a well defined energy and particle number, since generally E^* is not exchanged with the surrounding heat baths due to the short range nature of nuclear force. According to the MCE treatment, the number of accessible states $\Omega(E)$ is proportional to the density of states, i.e., to the experimental NLD $\rho(E)$, and hence the entropy (S) is given as [50]

$$S = k_B \ln \Omega(E) = k_B \ln \frac{\rho(E)}{\rho_0} = k_B \ln \rho(E) + S_0 \,, \quad (1)$$

where k_B is Boltzmann constant and ρ_0 is a normalization factor that ensures the validity of the third law of thermodynamics, i.e., $S \to 0$ for $T \to 0$. The factor S_0 is generally obtained using the ground-state energy band and adjusted to satisfy the third law of thermodynamics (see e.g., Ref. [37]). It should be mentioned that the value of S_0 is not much significant while calculating the entropy difference between two consecutive nuclei. Moreover, the variations in entropy on a linear scale with E^* are equivalent to the variations in the level density on a logarithmic scale (Figs. 1 and 2) and therefore, the MCE entropy is not shown separately.

The experimental proton entropy excess ΔS_p between ^{211}Po and ^{212}At ($\Delta S_p = S$ (^{211}Po) $-$ S (^{212}At)) is shown in Fig. 3(a), including also the low-energy data taken from RIPL-3 averaged over the angular-momentum distribution as in Ref. [10]. It is important to point out that the angular momentum does not have any effect while taking the difference in entropy as both nuclei have almost similar angular-momentum distribution. Fig. 3(a) clearly indicates that the experimental ΔS_p value decreases with increasing E^* and becomes almost constant ($\sim$0.5 k_B) as $E^* > 3$ MeV, which is much smaller than that obtained earlier due to the single neutron

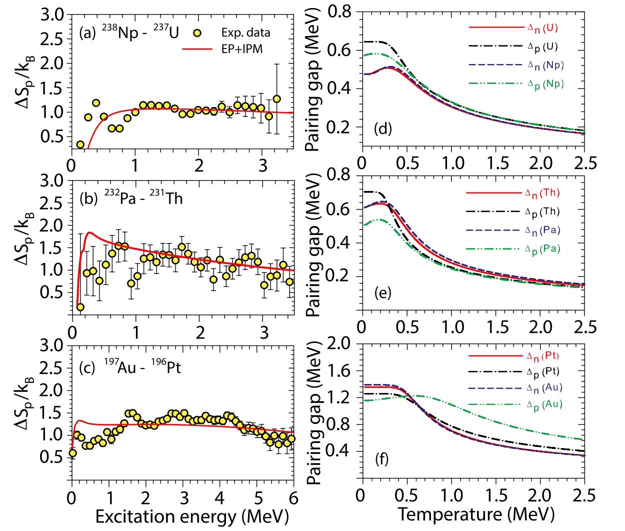

Fig. 4. The same as in Fig. 3 but for different sets of nuclei. Exp. data in (a), (b), and (c) are obtained by using the corresponding NLD data in Figs. 2[(d), (c), and (b)], respectively.

($\sim$1.3 $-$ 2 k_B) [35,37–39]. At $E^* \sim 1.0$ MeV, there seems to appear a deep valley of the experimental ΔS_p curve for the ^{211}Po–^{212}At set [Fig. 1(a)], whereas that for the ^{91}Zr–^{90}Y set [Fig. 1(b)] does not exhibit clearly a peak-like or valley-like structure because of lacking the data below 1 MeV. Here, it is worthwhile to mention that the experimental NLD data in the very low-energy region are mostly achieved by counting the number of known (discrete) levels (within a fixed energy interval) in the experimental nuclear level scheme taken from the nuclear databases [51,52]. It is well-known that the NLD in this very low-energy region has strong statistical fluctuations. The reason is that according to the statistical and thermal physics, the relative energy fluctuation $\delta E/\bar{E}$ ($\bar{E}$ is the average energy integrated by all possible energy states) is approximately related to $1/\sqrt{N}$ (N is the number of possible states) [53]. When δE becomes comparable with $\bar{E}$, temperature cannot be measured exactly. This happens when N is not so large, N decreases as T goes to 0, leading to the increase in the relative energy fluctuation. Obviously, in the very low-energy region, the number of known excited states in atomic nuclei is rather small, so energy and temperature in this region are strongly fluctuated. Hence, the experimental proton entropy excess in this very low-energy region also fluctuates. Nevertheless, it can easily be seen in Figs. 3(a) and (b) that the EP+IPM can reproduce the overall behavior of the experimental ΔS_p data. Moreover, there is a sharp peak at $E^* \sim 1.0$ MeV in the ΔS_p curve obtained within the EP+IPM for both two sets of nuclei in Fig. 3. The appearance of this peak is associated with the pairing reentrance phenomenon caused by the odd nucleon within the EP+IPM. This phenomenon can be seen via the exact neutron Δ_n and proton Δ_p pairing gaps obtained within the EP+IPM in Figs. 3(c) and (d). In Fig. 3(c), the neutron gaps slightly increase with low $T < 1$ MeV and rapidly decrease with $1 < T < 3$ MeV, above which their decrease becomes much slower. The increase in Δ_n at $T < 1$ MeV, which is known as a signature of the pairing reentrance phenomenon in hot nuclei, can be explained by the weakening of the blocking effect caused by the odd neutron at a temperature or excitation energy well below the value at which the first nucleon (Cooper) pair starts to break (leading to a rapid decrease of the pairing gap) [21,13]. The enhancement (reentrance) of Δ_n in ^{211}Po ($N = 127$) is stronger than that in ^{212}At ($N = 127$) as seen in Fig. 3(c) because the difference between the energies of the last occupied level and the level occupied by odd neutron $\delta\epsilon_n$ in the single-particle spectra of ^{211}Po ($\sim$3.512 MeV) is larger than that in ^{212}At ($\sim$2.816 MeV). Due to this phenomenon, the NLD of ^{211}Po at low $E^* < 1$ MeV is strongly enhanced as compared to that of ^{212}At, resulting in a pronounced peak in ΔS_p seen in Fig. 3(a). The proton pairing gap Δ_p of ^{212}At ($Z = 85$) also increases at very low $T < 0.4$ MeV but its increase is invisible because the value of $\delta\epsilon_p$ (similar to $\delta\epsilon_n$ but for proton) in ^{212}At is very small (∼0.381 MeV) and therefore, has negligible contribution to the enhancements of NLD as well as ΔS_p at low E^*. Similarly, a pronounced peak seen in the proton entropy excess obtained within the EP+IPM for two spherical ^{90}Y and ^{91}Zr nuclei at $E^* \sim 1$ MeV [Fig. 3(b)] can be also explained by the increase in their neutron pairing gaps caused by odd neutron or the pairing reentrance phenomenon at $T \sim 1$ MeV [Fig. 3(d)]. In this case, the values of $\delta\epsilon_n$ in ^{90}Y ($N = 51$) and ^{91}Zr ($N = 51$) are comparable (3.164 MeV for ^{90}Y and 3.213 MeV for ^{91}Zr), so the increases of their neutron pairing gaps at $T \sim 1$ MeV are similar. The proton entropy excess between ^{90}Y and ^{91}Zr is ∼0.5 k_B at $E^* \sim 3$ MeV, similar to that between ^{211}Po and ^{212}At, and slowly decreases to reach ∼0.1 k_B at $E^* > 3$ MeV.

In order to further understand the proton entropy excess, the entropy difference has been studied in other mass region with high deformations. It is seen in Figs. 4[(a)-(c)] that peak-like structures are also seen in the EP+IPM calculations for these sets of heavy-mass and well-deformed nuclei. However, these peaks are rather weak and located at very low $E^* \sim 0.2 - 0.4$ MeV, whereas the experimental curves exhibit strong fluctuations in this energy region. The reason of these weak low-energy peaks seen in the EP+IPM might be due to the fact that although the pairing reentrance is seen in the neutron and proton pairing gaps in Figs. 4[(d)-(f)], their absolute values are smaller than those in Figs. 3[(c)-(d)], which weakly affect the NLDs and proton entropy excesses. Moreover, the proton entropy excess in these systems is around $\sim 1.0 - 1.2$ k_B, which is much larger than that in spherical ^{211}Po–^{212}At and ^{90}Y–^{91}Zr systems ($\sim 0.1 - 0.5$ k_B). This is possibly due to the nuclear deformation. The spherical systems are generally more stable with external temperature or excitation than the deformed ones. As the result, the entropy of spherical systems hardly changes as compared to that of the deformed ones. In addition, the smaller proton entropy excess could also be due to the shell effect since ^{211}Po and ^{212}At are near the double shell closure, while ^{90}Y and ^{91}Zr are near the neutron shell closure. The valence particle around the shell closure carries lower entropy due to the limited number of quantum states available for the system [6]. The present study also reveals that the proton entropy excess is notably smaller ($\sim 0.1 - 1.2$ k_B) than the neutron one ($\sim 1.3 - 2.0$ k_B). This is because the proton Fermi surface lies at a lower energy than that of neutron (due to the Coulomb interaction) and the single proton orbitals have lower density than those of neutrons. Therefore, the protons do not have so many available orbitals contributing to the level density. These interesting observations clearly highlight that proton carries less entropy as compared to neutron.

In summary, the entropy excess caused by a single proton (proton entropy excess) ΔS_p between different sets of spherical and deformed nuclei has been investigated based on the available nuclear level density data. It is found that the experimental value of ΔS_p as a function of E^* exhibits a strong fluctuation at $E^* < 1$ MeV and reaches saturation at high $E^* > 3 - 6$ MeV. The analysis within the microscopic EP+IPM calculations shows that the proton entropy excess is $\sim 0.1 - 0.5$ k_B for the spherical systems and $\sim 1.0 - 1.2$ k_B the deformed ones, in good agreement with the experimental data. This value of proton entropy excess is smaller than that of the neutron one due to the effect of Coulomb interaction and proton single-particle level density, which is less than the neutron one. Moreover, a peak-like structure, which is seen in the proton entropy excess obtained within the EP+IPM at low energy $E^* < 1$ MeV, is explained by the pairing reentrance phenomenon caused by the weakening of blocking effect of an odd nucleon. This peak-like structure is found to be more pronounced in the spherical systems than in the deformed ones because the pairing reentrance is stronger in spherical nuclei than in deformed ones. However, this theoretical peak-like structure is not well supported by the experimental observation due to the strong fluctuations of the measured data. Therefore, more precise and direct experimental measurements in the low-energy region ($E^* < 1$ MeV) are called in order to confirm our theoretical predictions.

Declaration of competing interest

The authors declare that they have no known competing financial interests or personal relationships that could have appeared to influence the work reported in this paper.

Acknowledgement

Balaram Dey would like to thank Prof. Magne Sveen Guttormsen, Department of Physics, University of Oslo, Norway for the useful discussions and suggestions on the subject of investigation. This work is funded by the National Foundation for Science and Technology Development (NAFOSTED) of Vietnam through Grant No. 103.04-2019.371.

References

[1] J.M. Lattimer, Annu. Rev. Nucl. Part. Sci. 31 (1981) 337.
[2] N.K. Glendenning, Phys. Rep. 342 (2001) 393.
[3] G. Steigman, Annu. Rev. Nucl. Part. Sci. 57 (2007) 463.
[4] E.O. Zavarygin, A.V. Ivanchik, J. Phys. Conf. Ser. 661 (2015) 012016.
[5] A. Schiller, et al., Phys. Rev. C 63 (2001) 021306(R).
[6] M. Guttormsen, M. Hjorth-Jensen, E. Melby, J. Rekstad, A. Schiller, S. Siem, Phys. Rev. C 63 (2001) 044301.
[7] K. Kaneko, M. Hasegawa, Nucl. Phys. A 740 (2004) 95.
[8] K. Kaneko, et al., Phys. Rev. C 74 (2006) 024325.
[9] Balaram Dey, et al., Phys. Rev. C 96 (2017) 054326.
[10] Balaram Dey, et al., Phys. Lett. B 789 (2019) 634.
[11] Thi Quynh Huong Le, Dong Xuan Tran, Ngoc Anh Nguyen, Quang Hung Nguyen, Eur. Phys. J. A 57 (2021) 109.
[12] J. Margueron, E. Khan, Phys. Rev. C 86 (2012) 065801.
[13] N. Quang Hung, N. Dinh Dang, L.T. Quynh Huong, Phys. Rev. C 94 (2016) 024341.
[14] M.M. Belabbas, J.J. Li, J. Margueron, Phys. Rev. C 96 (2017) 024304.
[15] R. Balian, H. Flocard, M. Veneroni, Phys. Rep. 317 (1999) 251.
[16] S. Frauendorf, N.K. Kuzmenko, V.M. Mikhajlov, J.A. Sheikh, Phys. Rev. B 68 (2003) 024518.
[17] N. Quang Hung, N. Dinh Dang, Phys. Rev. C 78 (2008) 064315.
[18] D.J. Dean, K. Langanke, H.A. Nam, W. Nazarewicz, Phys. Rev. Lett. 105 (2010) 212504.
[19] N. Quang Hung, N. Dinh Dang, Phys. Rev. C 84 (2011) 054324.
[20] N. Quang Hung, N. Dinh Dang, B.K. Agrawal, V.M. Datar, A. Mitra, D.R. Chakrabarty, Acta Phys. Pol. B, Proc. Suppl. 8 (2015) 551.
[21] N. Quang Hung, N. Dinh Dang, L.G. Moretto, Rep. Prog. Phys. 82 (2019) 064322.
[22] T. Kammuri, Prog. Theor. Phys. 31 (1964) 595.
[23] L.G. Moretto, Phys. Lett. B 35 (1971) 379.
[24] L.G. Moretto, Nucl. Phys. A 185 (1972) 145.
[25] P. Bonche, S. Levit, D. Vautherin, Nucl. Phys. A 427 (1984) 278.
[26] B.K. Agrawal, Tapas Sil, J.N. De, S.K. Samaddar, Phys. Rev. C 62 (2000) 044307.
[27] B.K. Agrawal, Tapas Sil, S.K. Samaddar, J.N. De, Phys. Rev. C 63 (2001) 024002.
[28] A.L. Goodman, Phys. Rev. C 34 (1986) 1942.
[29] J.L. Egido, L.M. Robledo, V. Martin, Phys. Rev. Lett. 85 (2000) 26.
[30] S.E. Koonin, D.J. Dean, K. Langanke, Phys. Rep. 278 (1997) 1.
[31] S. Liu, Y. Alhassid, Phys. Rev. Lett. 87 (2001) 022501.
[32] N. Quang Hung, N. Dinh Dang, L.T. Quynh Huong, Phys. Rev. Lett. 118 (2017) 022502.
[33] N. Quang Hung, N. Dinh Dang, L. Tan Phuc, N. Ngoc Anh, T. Dong Xuan, T.V. Nhan Hao, Phys. Lett. B 811 (2020) 135858.
[34] E. Melby, M. Guttormsen, J. Rekstad, A. Schiller, S. Siem, A. Voinov, Phys. Rev. C 63 (2001) 044309.
[35] M. Guttormsen, et al., Phys. Rev. C 88 (2013) 024307.
[36] F. Giacoppo, et al., Phys. Rev. C 90 (2014) 054330.
[37] M. Guttormsen, A. Bjerve, M. Hjorth-Jensen, E. Melby, J. Rekstad, A. Schiller, S. Siem, A. Belic, Phys. Rev. C 62 (2000) 024306.
[38] U. Agvaanluvsan, A.C. Larsen, M. Guttormsen, R. Chankova, G.E. Mitchell, A. Schiller, S. Siem, A. Voinov, Phys. Rev. C 79 (2009) 014320.

[39] E. Algin, U. Agvaanluvsan, M. Guttormsen, A.C. Larsen, G.E. Mitchell, J. Rekstad, A. Schiller, S. Siem, A. Voinov, Phys. Rev. C 78 (2008) 054321.
[40] A. Schiller, et al., Nucl. Instrum. Methods A 447 (2000) 498.
[41] Pratap Roy, et al., Phys. Rev. C 94 (2016) 064607.
[42] M. Guttormsen, et al., Phys. Rev. C 90 (2014) 044309.
[43] M. Guttormsen, et al., Phys. Rev. C 96 (2017) 024313.
[44] M. Guttormsen, et al., Phys. Rev. C 89 (2014) 014302.
[45] T.G. Tornyi, et al., Phys. Rev. C 89 (2014) 044323.
[46] S. Cwiok, J. Dudek, W. Nazarewicz, J. Skalski, T. Werner, Comput. Phys. Commun. 46 (1987) 379.
[47] P. Moller, A.J. Sierk, T. Ichikawa, H. Sagawa, At. Data Nucl. Data Tables 109–110 (2016) 1.
[48] N. Dinh Dang, N. Quang Hung, L.T. Quynh Huong, Phys. Rev. C 96 (2017) 054321.
[49] N. Ngoc Anh, N. Quang Hung, N. Xuan Hai, P. Dinh Khang, A.M. Sukhovoj, L.V. Mitsyna, H. Huu Thang, L. Hong Khiem, Phys. Rev. C 100 (2019) 023324;
N. Ngoc Anh, N. Quang Hung, N. Xuan Hai, P. Dinh Khang, A.M. Sukhovoj, L.V. Mitsyna, H. Huu Thang, L. Hong Khiem, Phys. Rev. C 102 (2020) 019906(E).
[50] A. Bohr, B.R. Mottelson, Nuclear Structure, Vol. I, Benjamin, New York, 1969.
[51] https://www-nds.iaea.org/RIPL-3/.
[52] https://www-nds.iaea.org/public/ensdf_pgm/.
[53] F. Reif, Fundamentals of Statistical and Thermal Physics, Mc Grow-Hill, Singapore, 1964.